The Meteoritical Society

Meteoritics & Planetary Science 42, Nr 4/5, 779–792 (2007)
Abstract available online at http://meteoritics.org

Lithological and structural characteristics of the Lake Bosumtwi impact crater, Ghana: Interpretation of acoustic televiewer images

Sabine HUNZE[1, 2*] and Thomas WONIK[1]

[1]Institut für Geowissenschaftliche Gemeinschaftsaufgaben, Stilleweg 2, D-30655 Hannover, Germany
[2]Institut für Planetologie, Westfälische Wilhelms-Universität Münster, Wilhelm-Klemm-Str. 10, D-48149 Münster, Germany
*Corresponding author. E-mail: sabine.hunze@gga-hannover.de

(Received 21 September 2006; revision accepted 06 February 2007)

Abstract–Bosumtwi is a very well-preserved 1.07 Myr old, complex terrestrial impact crater located in south-central Ghana, West Africa. The impact structure has a diameter of about 10.5 km and was formed in 2.1–2.2 Gyr Precambrian metasedimentary and metavolcanic rocks. Drilling and logging was carried out during the Lake Bosumtwi Drilling Project (BCDP) which was supported by the International Continental Scientific Drilling Program (ICDP). One of the aims of this project is to achieve detailed information on the subsurface structure and crater fill of one of the best preserved large young impact structures.

We interpreted the wireline logs and televiewer images. The physical properties including shallow resistivity, p-wave velocity, magnetic susceptibility, and borehole diameter of the breccia differ significantly from those of the meta-graywackes and slate/phyllites. Fractures observed in the televiewer images are interpreted to determine their characteristic structural features. The fracture dip angles are steep (50–70°) and the two main dip directions are southeast and southwest. Most fractures observed in the borehole are open. The indicated main stress direction is north-south.

INTRODUCTION

Geology

The 1.07 Myr Bosumtwi crater (centered at 06°30′N and 01°25′W) is situated in the Ashanti Region of Ghana, West Africa, and is centered about 32 km east of Kumasi, the regional capital (Fig. 1). It is a well-preserved, complex terrestrial impact structure that displays a pronounced rim and is almost completely filled by Lake Bosumtwi. The crater has a rim-to-rim diameter of about 10.5 km and is formed in 2.1–2.2 Gyr, lower greenschist facies metasediments of the Birimian Supergroup (Junner 1937). These rocks mainly contain meta-graywackes, phyllites, and quartzites together with shales and slates (Jones et al. 1981; Leube et al. 1990). The deformational event and deposition of the Tarkwaian Supergroup followed Birimian sedimentation. Tarkwaian coarse-grained clastic sedimentary rocks, which are regarded as the detritus of Birimian rocks (Leube et al. 1990), occur to the southeast of the crater (Plado et al. 2000). Recent rock formations include the Bosumtwi lake beds, and soils and breccias associated with the formation of the crater (e.g., Junner 1937; Reimold et al. 1998). Impact breccia units are subdivided into polymict breccia, suevite, monomict lithic breccia, and suevite dikes (Coney et al. 2006; Deutsch et al. 2006; Reimold et al. 2006). The regional geology is characterized by a strong, northeast-trending fabric with steep, subvertical dips to northwest and southeast (Reimold et al. 1998).

Drilling

The Lake Bosumtwi Drilling Project (BCDP) was supported by the International Continental Scientific Drilling Program (ICDP). Drilling at Lake Bosumtwi was carried out from July to October 2004. Wireline logging was conducted in October 2004. Two sites which contain core samples of the impact and crystalline basement lithologies were drilled: boreholes LB-07A and LB-08A (Fig. 2). Borehole LB-07A was drilled into the circular depression northwest of the central uplift. The upper section (70–360 m) contains lake sediments, the lower section (360–550 m) impact rocks. Borehole LB-08A was drilled into the shoulder of the central uplift. Here sediments were drilled from 70 to 238 m and impact rocks from 238 to 455 m. Our analysis focuses on borehole LB-08A because of the availability of televiewer

© The Meteoritical Society, 2007. Printed in USA.

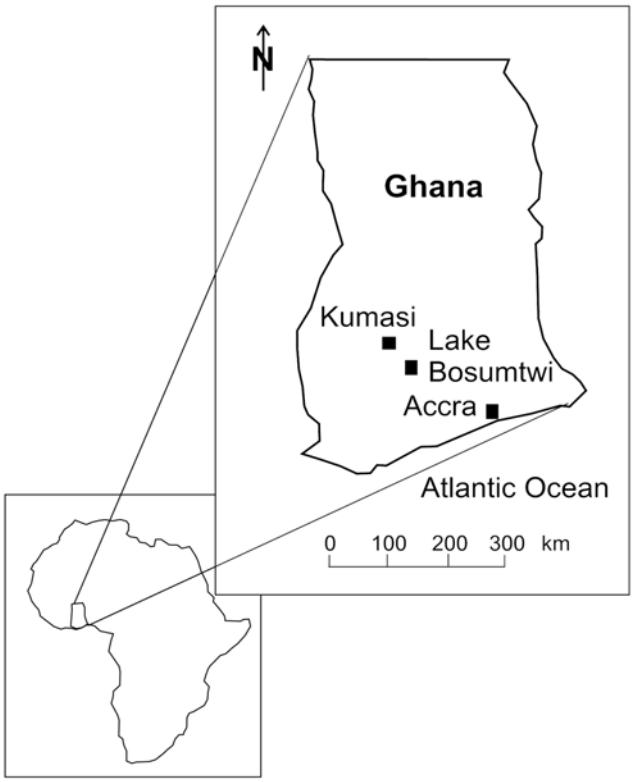

Fig. 1. The location of Lake Bosumtwi (Ghana) in western Africa (after Koeberl et al. 1997).

images, wireline logs, and core descriptions in the section with impact rocks.

The core recovery in borehole LB-08A from all 71 runs within the impact rocks was very high (average 96%). The summary core run report is given at the Lake Bosumtwi home page (http://www.icdp-online.de/contenido/icdp/front_content.php?idart=1117). Only 10 runs had a core recovery lower than 80%, while another 10 runs had core recoveries higher than 100% as a result of core dilation. The highest core recovery was 111%, the lowest 40%.

METHODS

Drilling

The Global Lake Drilling 800 m (GLAD800) system was developed to collect long continuous cores in lake sediments (for more details see the DOSECC web page (http://www.dosecc.org/html/body_glad800.html). The GLAD800 contains a transport system that includes a drilling rig and a modular barge. The drilling rig can operate from different flotation systems or can be used on land as a typical diamond core rig. The barge is suitable for core handling, preliminary description, marking, and temporary storage. The barge can be anchored in waters up to 200 m deep using anchoring or dynamic positioning systems. The rig collects core up to a depth of 800 m (water and sediment). The GLAD800 includes six standard tools and is termed the DOSECC Lake Coring System (DLS). The tools are similar to those used in the Ocean Drilling Program and in commercial geotechnical work. The DLS cuts a 5.50-inch (139.7-millimeter) diameter borehole. Core runs are designed to be 3 meters in length.

Logging

The cores with impact-related material were documented by geophysical logging (gamma-density and magnetic susceptibility) and detailed core descriptions. These descriptions were made at the ICDP headquarters at the GeoForschungsZentrum (GFZ) in Potsdam, Germany. Gamma density was measured at irregular intervals depending on the availability of suitable samples, which need a regular diameter and a flat surface. Magnetic susceptibility was measured approximately every 10 cm (Ugalde 2006).

Borehole logging is used to acquire continuous, fine-scale, in situ physical parameters within the borehole. Geophysical logging provides unique continuous lithological and structural data on the impact rocks. A set of petrophysical measurements can be obtained with the slimhole logging tools available from ICDP and GFZ: natural gamma ray spectrometry (potassium, thorium, and uranium), magnetic susceptibility, electrical resistivity (shallow penetration depth), p-wave velocity, and caliper (borehole diameter) (Fig. 3). In addition, 3-D magnetometer, 4-arm dipmeter, and acoustic televiewer logs were run.

Borehole Televiewer

The acoustic televiewer tool (from Antares Datensysteme GmbH, Televiewer Typ 1303) provides high-quality dip and azimuth measurements to investigate fractures, supply information on borehole breakouts, and give information on lithological boundaries, textures, and sedimentary features (Rider 1996). The tool string is approximately 3 m long. It is an acoustic device that provides an image of the surface reflectivity of the wall in a fluid-filled borehole (Zemanek et al. 1970). As the tool is pulled up the borehole, pulses fired in rapid sequence from an acoustic transducer are reflected from the wall of the borehole and returned to the transducer (Moos et al. 2000). At each sample point, the acoustic tool acquires a measurement of the travel time and the reflected amplitude. The travel or run time is the time between emission, reflection off the borehole wall, and detection back at the transducer. It varies with borehole geometry and is therefore sensitive to borehole ovality, which is used to identify borehole breakouts. The travel time is also affected by voids in the borehole wall such as open fractures which do not return signals (Rider 1996). The resulting log is

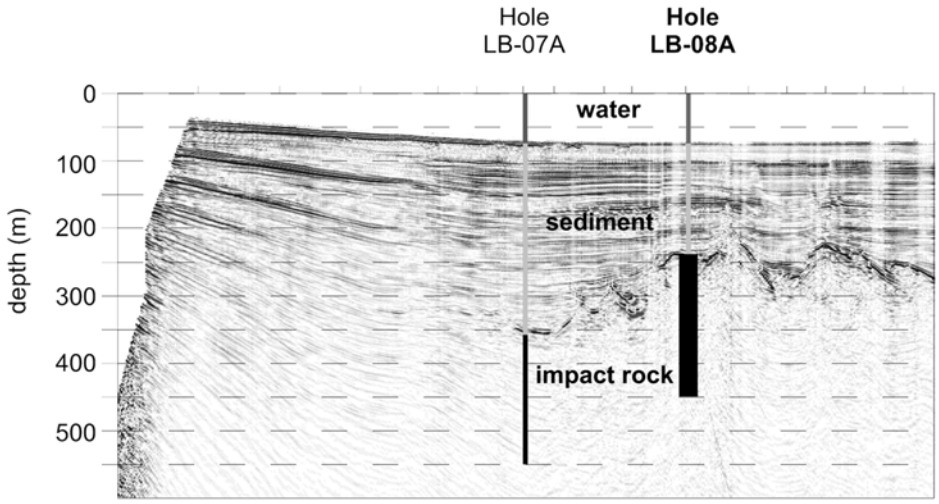

Fig. 2. A seismic reflection profile showing drilling locations of boreholes LB-07A and LB-08A (after Scholz et al. 2002). Depth section of a NW-SE seismic line across the lake center. The marked section of borehole LB-08A is analyzed in this paper. Vertical exaggeration 1:3.

a representation of the borehole wall as if it were split vertically along magnetic north and laid out flat (Zemanek et al. 1970). For example, a fracture plane that intersects the borehole wall at a given angle produces a sinusoidal trace on the televiewer log (Paillet et al. 1985).

Televiewer Data Quality

The acoustic televiewer data are of good quality because the deviation of the borehole does not exceed 5°. The deviation from vertical between the surface drill location and the total depth at 455 m is about 5 m northwest. The borehole has no azimuthal deviation down to 300 m; below this depth the deviation increases up to 5°. On average, the tool rotates every 20 m. The resulting loss in data quality is very small and can be ignored.

Dip and Strike Measurements

The GeoBase software (version 4.20, for details see http://www.antares-geo.de/english/software.html) created by Antares Datensysteme GmbH (Stuhr, Germany) was used to determine the dip and strike of fractures. The significant sinusoidal structures (e.g., fractures) were selected manually. For this purpose, a minimum of three data points along the fracture curve are determined, and the program then automatically calculates the dip and strike of the fracture.

Depth Shift

The comparison between televiewer images and core photos shows an average depth shift of 1.7 m. The shifts vary between 1.3 and 2.2 m. The depth shift is calibrated at breccia layers in the televiewer images and from core descriptions and core photos. The depth of the cores has to be corrected to correlate with the televiewer images and with the core photos. For this purpose, 1.7 m is added to the core depth to tie it into the televiewer depth.

The caliper values of the televiewer and the wireline logs were analyzed by comparing the depths of obvious breakouts. This revealed no significant depth shifts. The problem is that the caliper values of the wireline logs are measured mechanically by a three-arm caliper while those of the acoustic televiewer are calculated by acoustic travel time and velocity. The wireline caliper comprises two logs (C1 and C2) which differ significantly in some borehole sections. This possibly reflects borehole ovality caused by the regional tectonic stress field.

RESULTS

Lithology

Physical Properties

Borehole LB-08A is composed of target rocks (meta-graywacke and phyllite to slate) and impact breccia (allochthonous, dike, and autochthonous breccia [e.g., Deutsch et al. 2007]). The physical properties of each lithology are determined using the discriminance analysis statistical method calculated by the WINSTAT software (statistics for Windows). Selected, depth-limited sections of each lithology are chosen from the core descriptions as calibration sections. The discriminance analysis uses a set of independent variables, the wireline logs, and predicts the most probable match to a lithology (Backhaus et al. 1996; Schönwiese 2000). Here, each depth point is assigned to one of the three lithologies. The result is a synthetic continuous litho-log for the whole wireline log section (Fig. 3).

These three lithologies are plotted as box and whisker diagrams (Fig. 4). The physical parameters of the breccia

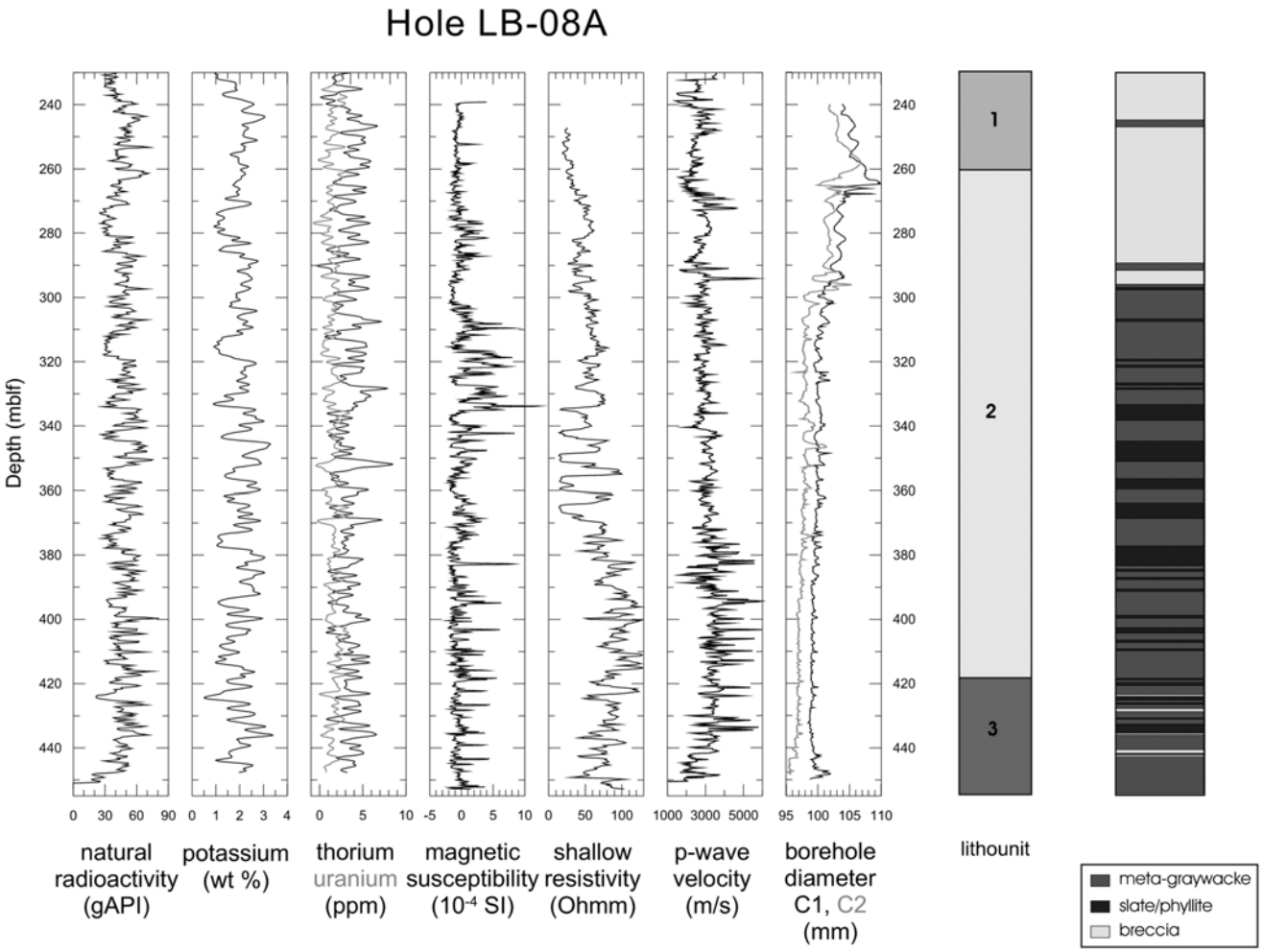

Fig. 3. An overview of wireline logs in borehole LB-08A in the 230–455 m depth interval. The unit of the natural radioactivity is gAPI (American Petroleum Institute gamma ray units). It was defined in a reference borehole at a site of the University of Texas. Also shows the three lithounits after Deutsch et al. (2007) and the litho-log derived from discriminance analysis. The lithology of lithounit 1 comprises melt-bearing allochthonous, polymict, and mostly clast-supported breccia. Lithounit 2 is composed of meta-graywackes alternating with phyllite to slate; few (par-)autochthonous breccia bodies and rare dike breccias are present. Lithounit 3 contains melt-bearing breccia dikes in country rocks identical to those occurring above (Deutsch et al. 2007).

differ significantly from those of the meta-graywacke and slate/phyllite. The breccia is characterized by the lowest resistivity and p-wave velocity and the highest borehole diameter values. In contrast, the natural radioactivity values of the breccia and the meta-graywackes are similar. This might be caused by the intrusion of breccia into the meta-graywacke host rock. Additionally, crossplots are used to analyze the physical properties of the three main lithologies: the p-wave velocity versus magnetic susceptibility crossplot (Fig. 5a) shows no obvious differentiation of the three lithologies, because their physical properties are quite similar. This might be due to the similar grain size of the three lithologies and comparable clay mineral and fluid contents.

The natural radioactivity versus shallow resistivity crossplot shows a better discrimination of the lithologies (Fig. 5b). Two data clusters can be separated by the shallow resistivity log: meta-graywackes with higher values (60–120 Ωm) and breccias with lower values (20–50 Ωm). Slates/phyllites show a wider data scatter, with resistivity values between 20 and 100 Ωm.

The p-wave velocity versus borehole diameter crossplot (Fig. 5c) shows a suitable lithological differentiation. Breccias show high borehole diameters and low p-wave velocities (<3000 m/s). There are also breccias with low borehole diameters (<100 mm) and medium to high p-wave velocities (3000 to 6000 m/s). One explanation for these two different data sets might be that the breccia intrudes into the meta-graywackes causing data from adjacent meta-graywackes to be included in the crossplot. Meta-graywacke is characterized by low borehole diameters and low to high p-wave velocities. Some meta-graywacke shows an enlarged borehole diameter (higher than the drilled borehole diameter

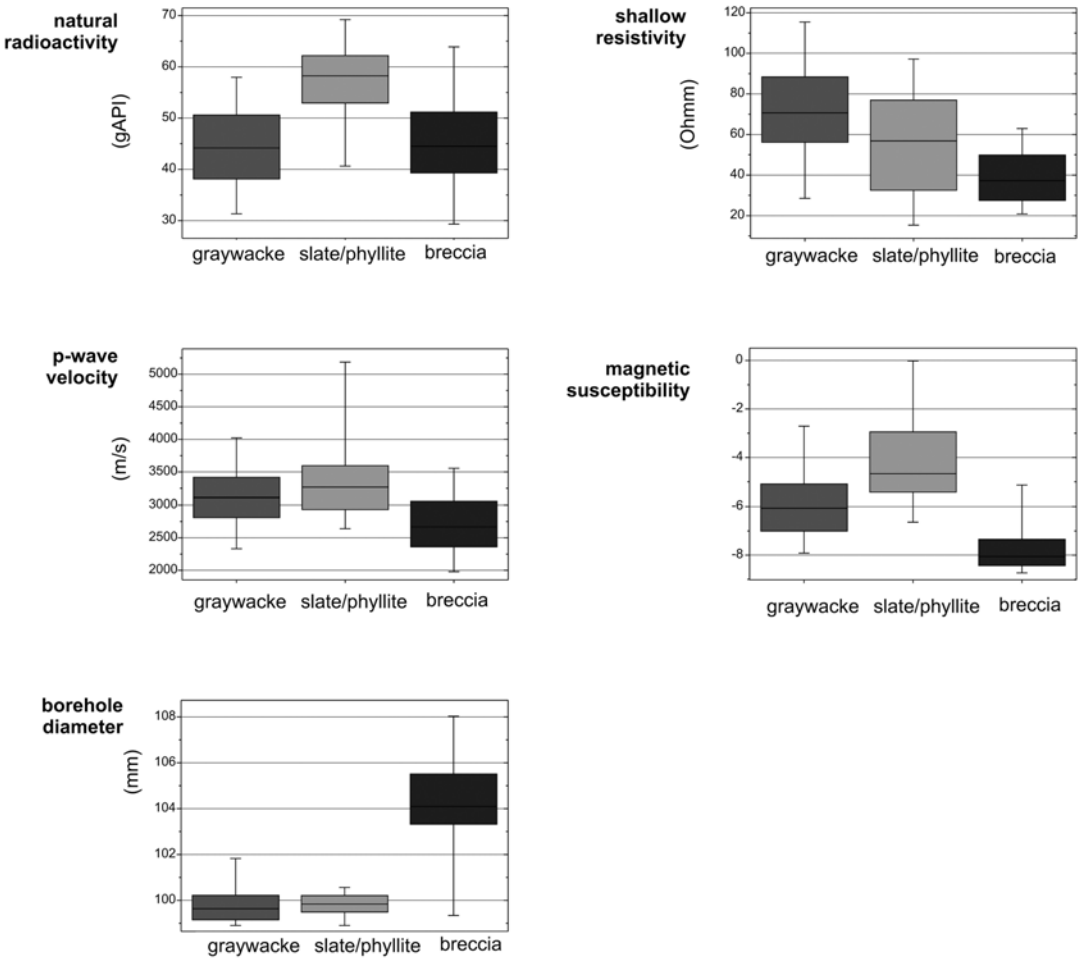

Fig. 4. Box and whisker diagrams of natural radioactivity, shallow electrical resistivity, p-wave velocity, and borehole diameter differentiated by lithologies determined from discriminance analysis. In the box and whisker diagrams the median is marked as horizontal line, the 25 and 75 percentiles as rectangle, and the 5 and 95 percentiles as lines. The depth sections of the lithounits are shown in Fig. 3.

of 95 mm) and low to medium p-wave velocities. They might be caused by a mixture of meta-graywacke and slate/phyllite. The properties of slate/phyllite lie between the two other lithologies and are characterized by medium to large borehole diameters and p-wave velocities. A possible reason for these observations might be that the borehole diameter depends on competence or rock lithification.

The natural radioactivity versus magnetic susceptibility crossplot shows rather good lithological differentiation (Fig. 5d). Breccia is characterized by lower magnetic susceptibilities. Meta-graywackes and slates/phyllites can be differentiated by their natural radioactivity values, which are higher in slate/phyllite (20–50 gAPI) than in meta-graywackes (50–70 gAPI).

Lithology and Televiewer Images

Acoustic impedance contrasts are used to differentiate the drilled lithologies. The characteristic features of the televiewer images for each lithology are described as follows: sections consisting exclusively of meta-graywacke occur, for example, at core depths 268.5–280.1 m, 312.9–318.7 m, 339.3–345.3 m, and 409.9–417.9 m. The televiewer images are characterized by a smooth and undisturbed appearance (Fig. 6). Only a few structures or irregularities, as well as sporadic fractures, are observed in the amplitude and run-time logs.

There are no sections with a relevant thickness (several meters) of pure slate/phyllite observed in the cores. However, sections with interbedded slate/phyllite and meta-graywacke occur, for example, at 331.9–336.1 m, 375.8–381.9 m, and 403–408 m. Two types of sections are identified from televiewer images: sections characterized by a smooth appearance without irregularities, and sections with an irregular appearance containing fractures and affected by core fragmentation (Fig. 7).

The presence of impact breccia is determined by their characteristic signature in the televiewer amplitude log: small-scale features (fine-grained matrix) and medium-scale features (coarse-grained clasts) (Fig. 8). The amplitude log

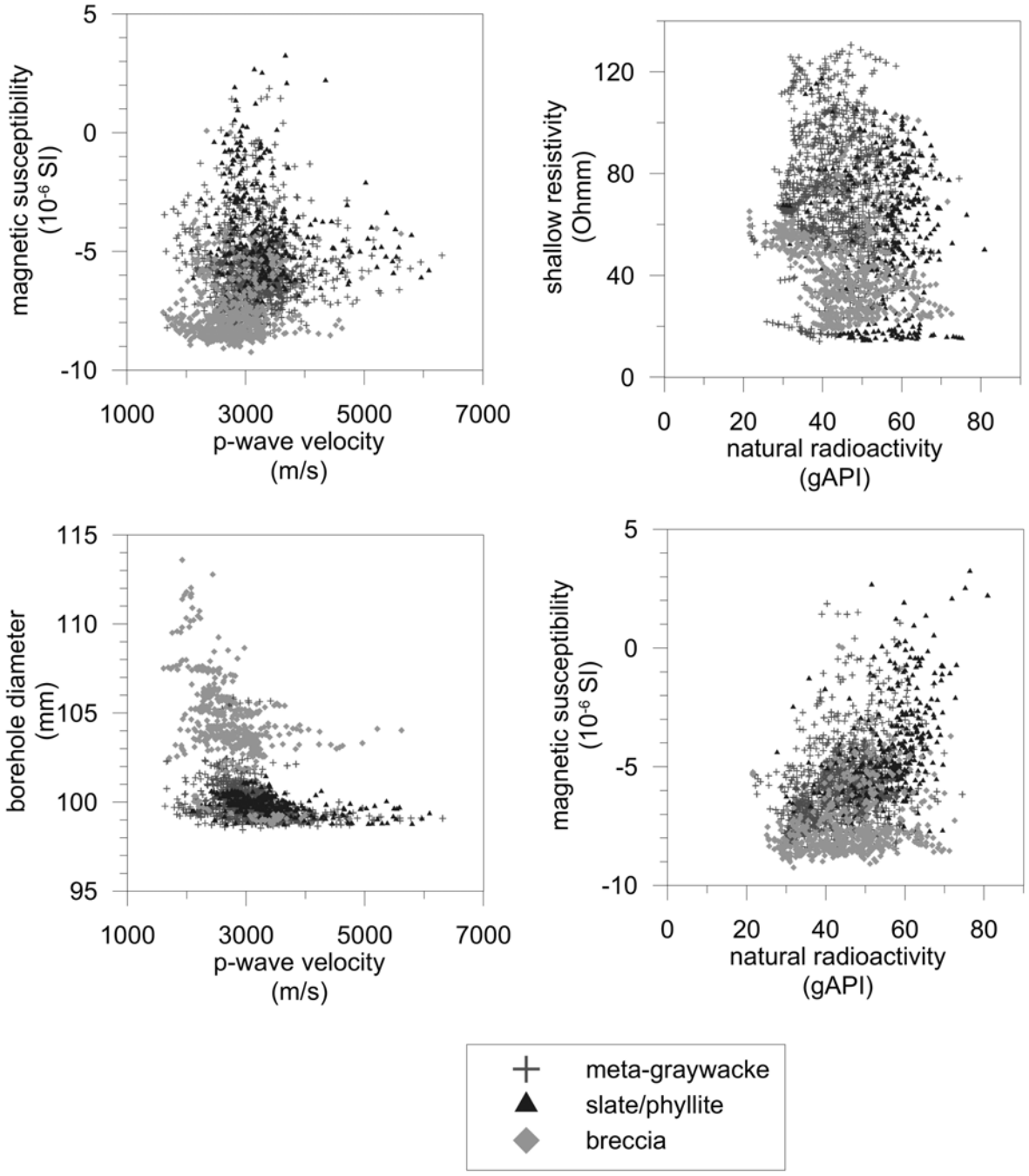

Fig. 5. Crossplots: (a) natural radioactivity versus shallow electrical resistivity, (b) p-wave velocity versus borehole diameter, (c) shallow resistivity versus p-wave velocity, (d) magnetic susceptibility versus shallow resistivity, (e) natural radioactivity versus magnetic susceptibility, and (f) shallow resistivity versus p-wave velocity. The lithologies are determined by discriminance analysis.

looks surprisingly similar to a core photo of the breccia. But the three types of breccia differentiated in the cores (allochthonous, autochthonous, and dike breccia) (cf. e.g., Deutsch et al. 2007) cannot be unambiguously identified in the televiewer images. There are differences in layer thicknesses between allochthonous and dike breccias (Fig. 9). The layer thickness of allochthonous breccias is higher (one meter to several meters) than dike breccias (one decimeter up to a meter). The grain size of the clasts is relatively larger in the allochthonous breccias. Detailed core descriptions and microscopic analysis are required for more precise breccia differentiation.

Borehole and Lithology

This raises the question of to what extent the specific lithology influences (a) the occurrence of fractures, (b) the

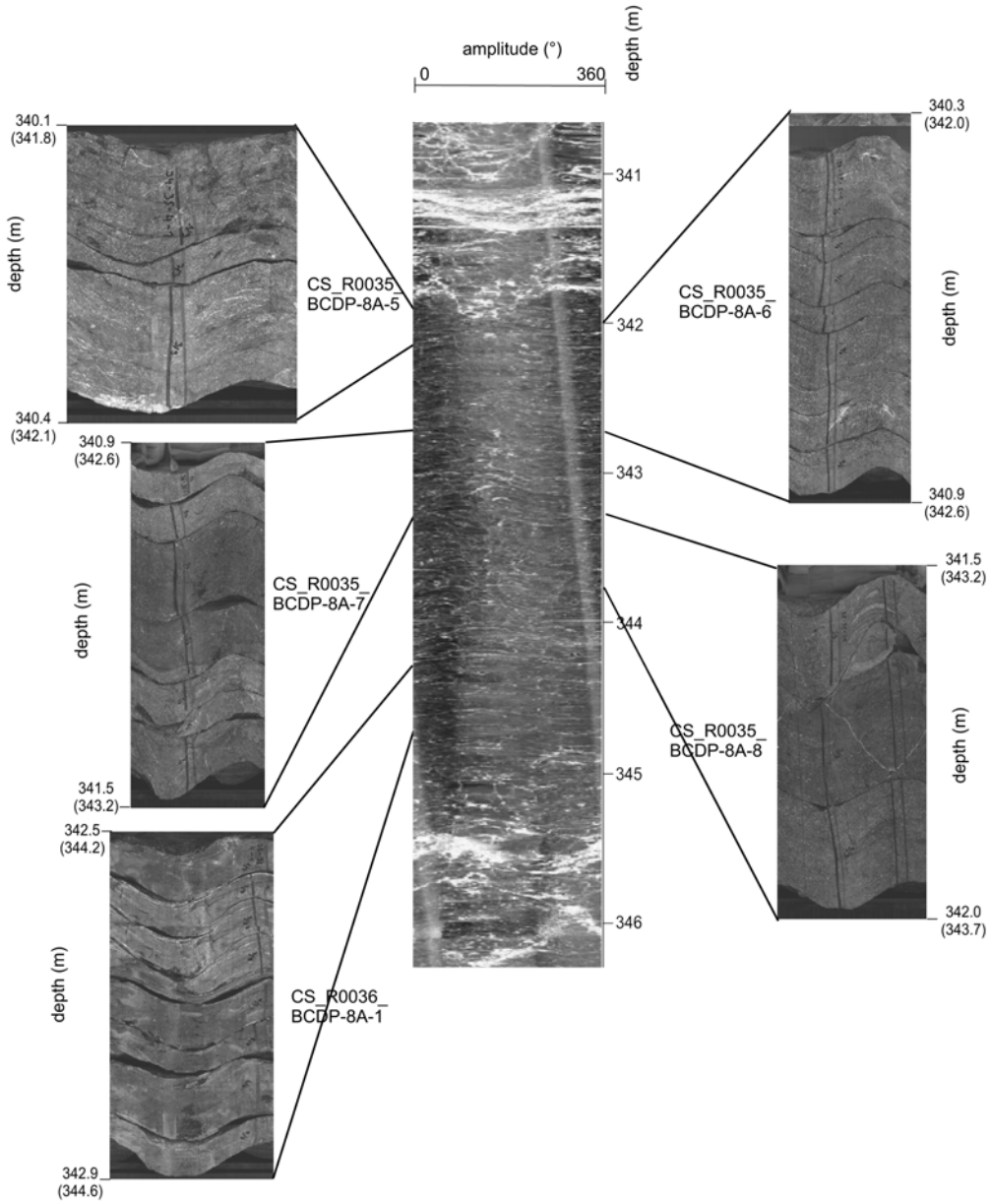

Fig. 6. A televiewer image of meta-graywacke and core photos of unrolled core scans. The detailed core photos are taken from the ICDP home page (http://www.icdp-online.de/contenido/icdp/front_content.php?idart=1118). For example, CS_R0035_BCDP-8A-5 means that this core photo is an unrolled core scan (CS), which was taken from Run 35 (R0035) of borehole BCDP-8A. The picture number is 5. Next to each core segment the depth of top and bottom and the televiewer depth (in brackets, depth shift +1.7 m) are given.

shape of the borehole, and (c) the degree of fragmentation. a) Most fractures occur in meta-graywacke, although rare fractures are also observed in slate/phyllite and breccia. This indicates that fractures develop easier and/or are better detected in more highly lithified units. b) Sections with an enhanced borehole diameter coincide with the occurrence of breccia. This correlation is not unambiguous, because slate/phyllite and meta-graywacke occasionally also have large borehole diameters (Fig. 5a). Sections with low core recovery occur at 260.0–269.1 m (40–77%), 284.4–296.6 m (67–88%), 333.1–339.2 m (63–82%), 366.7–372.8 m (61–85%), and 442.9–445.9 m (43%). They are composed of meta-graywacke with small amounts of breccia and slate/phyllite. Their televiewer images are characterized by an irregular appearance and a varying number of open fractures with different apertures. This often enables breccia layers, which are generally thin (<1 m), to be recognized. (c) Televiewer images of sections with highly fragmented material are characterized by an irregular appearance and a large number of fractures (Fig. 10). The corresponding cores consist of meta-graywacke,

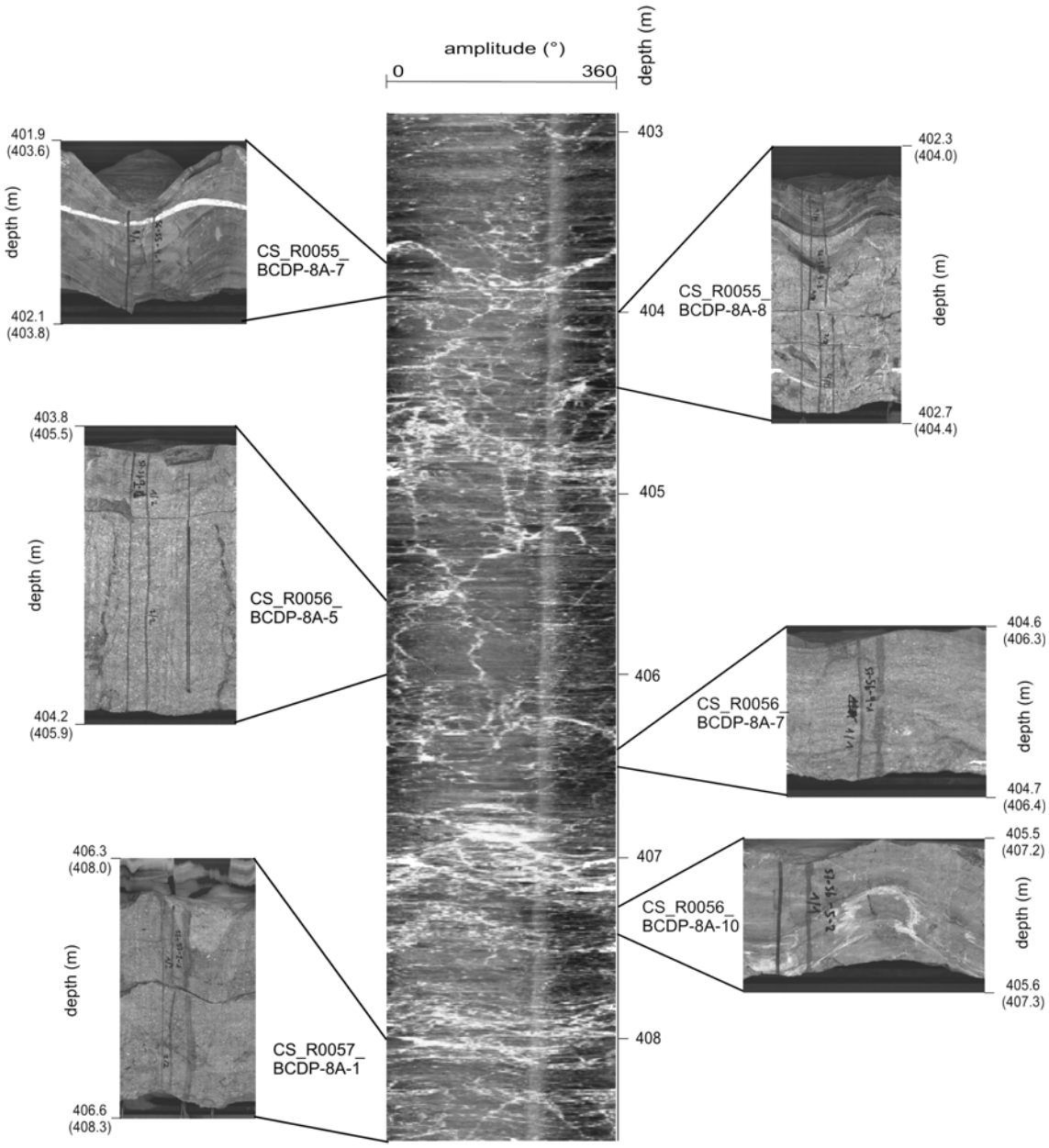

Fig. 7. Televiewer images of slate/phyllite and core photos of unrolled core scans. An explanation for the core scan abbreviation is given in Fig. 6. Next to each core segment the depth of top and bottom and the televiewer depth (in brackets, depth shift +1.7 m) are given.

slate/phyllite with meta-graywacke, and rare breccia. The fragmentation itself is observed in the televiewer images as a loss of signal, giving rise to a white-colored amplitude log. The fragmentation is possibly primarily caused by drilling in less lithified material. In contrast, those sections with intact cores (predominantly without fragmentation) show very smooth and undisturbed televiewer images, only few small-scale fractures, and only rarely borehole problems such as irregular vertical stripes in the televiewer amplitude log. The lithologies in the corresponding cores are composed of meta-graywacke and minor breccia.

Structural Geology

Fractures

Fractures observed in the televiewer images are characterized by a white signal in the amplitude and run-time logs and significant borehole enlargements (Fig. 11). Serra and Serra (2003) postulated that fractures appear on the caliper curve as either (a) a reduction in hole diameter in compacted zones which are in gauge, most probably due to a deposit of mud cake, especially if lost-circulation material has been used, or (b) an increase in hole diameter due to

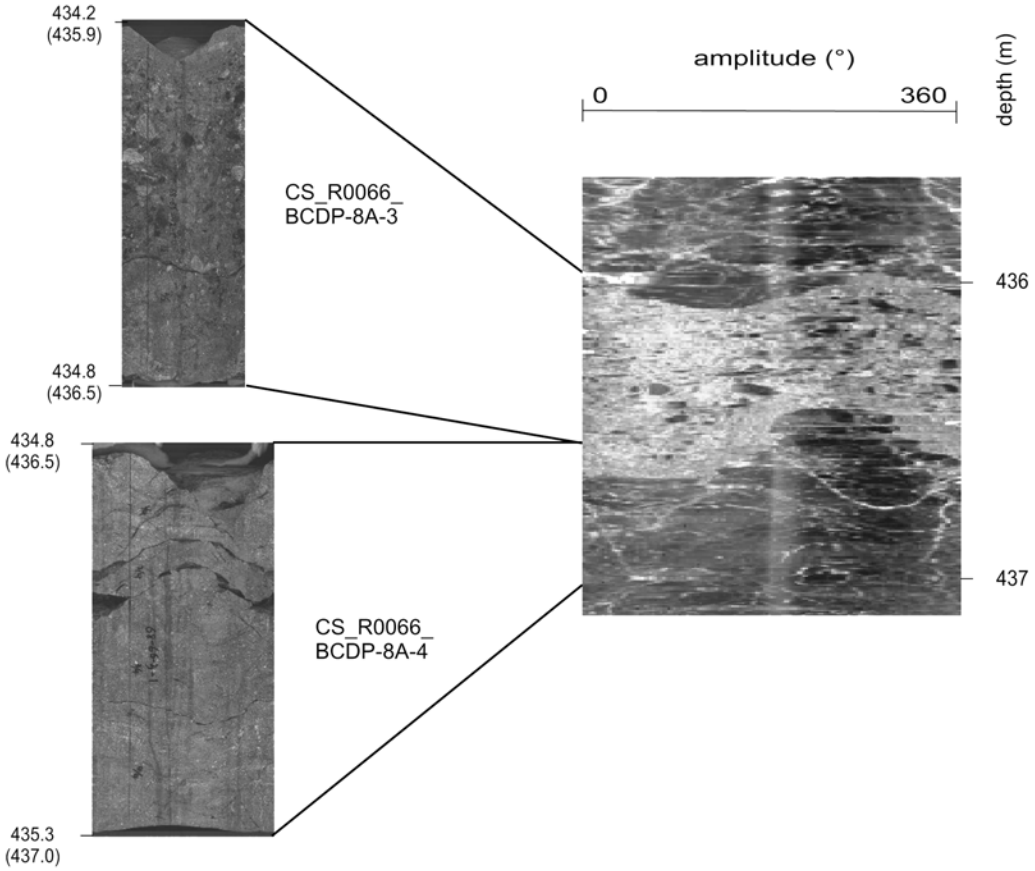

Fig. 8. Televiewer images of breccia and core photos of unrolled core scans. An explanation for the core scan abbreviation is given in Fig. 6. Next to each core segment the depth of top and bottom and the televiewer depth (in brackets, depth shift +1.7 m) are given.

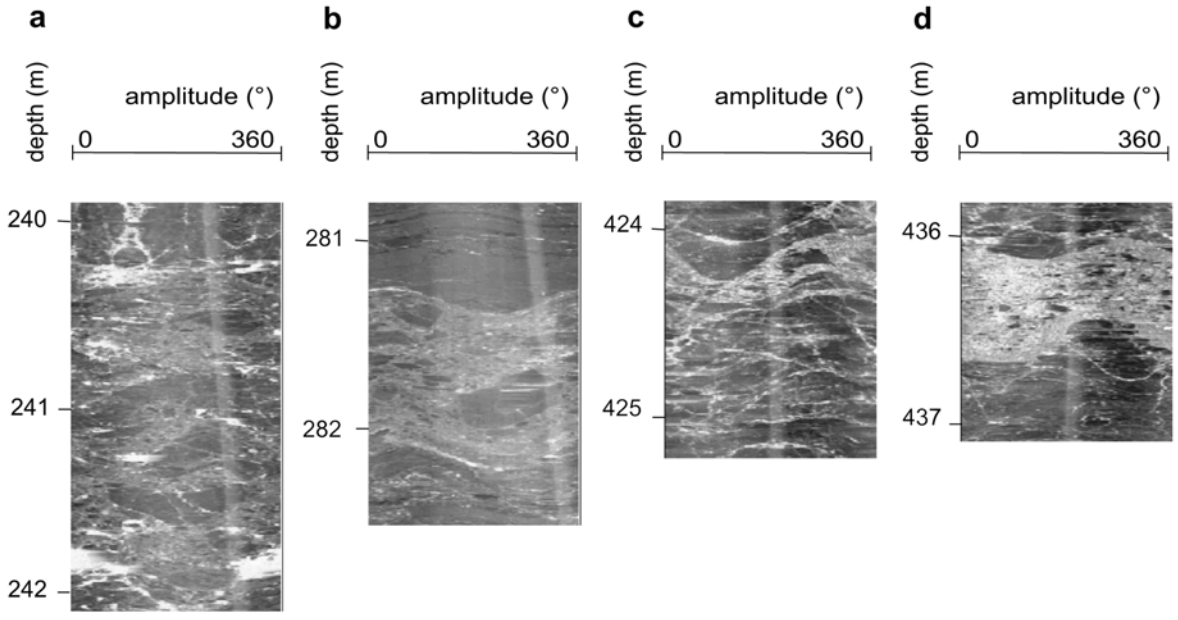

Fig. 9. Different appearance of impact breccia in the televiewer images. The two first examples (a, b) are allochthonous breccias; the other two (c, d) are dike breccias.

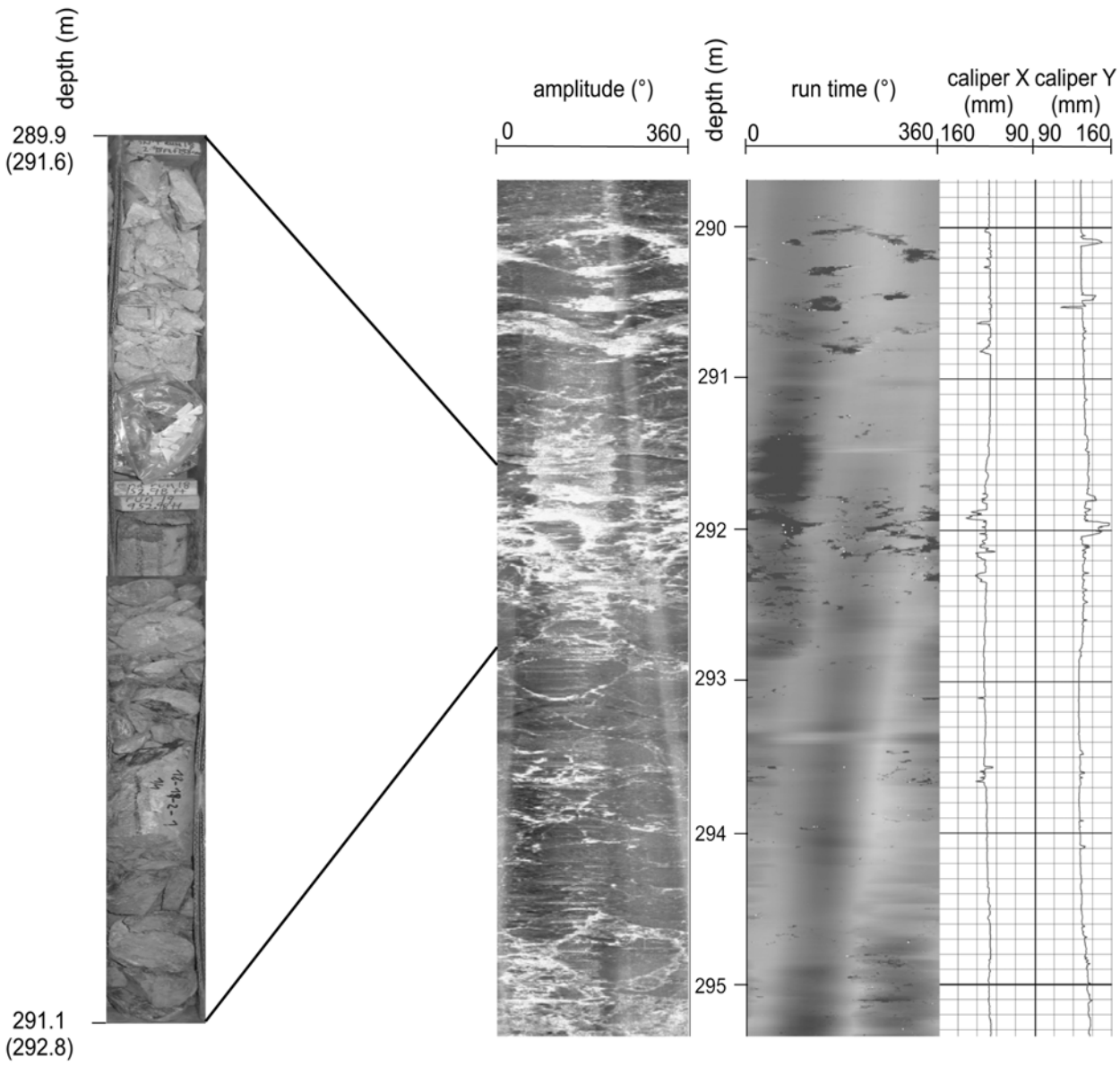

Fig. 10. A televiewer image (amplitude and run-time logs) and caliper logs of a fragmented core with a detailed core photo of core box 18 (depth 289.3–291 m, sections 1 and 2). Next to each core segment the depth of top and bottom and the televiewer depth (in brackets, depth shift +1.7 m) are given.

crumbling of the fractured zone during drilling causing chunks of various sizes to cave into the borehole.

Open and closed fractures are detected by comparing the televiewer amplitude and run-time logs. An open fracture gives a response through a loss of signal on the amplitude log, and also on the run-time log. A filled or closed fracture will provide an image on the amplitude log but no image on the run-time log (Taylor 1991). In borehole LB-08A, most fractures are open or partly open, and their signature is observed in both televiewer logs (Fig. 11a). But also closed and possibly mineralized fractures occur, for example, at televiewer depths 242 m, 262 m, 340 m, and 398.5 m (Fig. 11b).

Only about half of the fractures observed in the cores are also recognized in the televiewer images. The recognized fractures are characterized by a large aperture (0.05–0.15 m) or a high dip angle (>50°) with a small aperture (0.01–0.02 m). This difference in fracture identification between the televiewer images and the cores may be attributed to drilling-induced damage in the borehole, differences in scale and resolution, depth shift errors in both core and logs, or the limited resolution of the tool (Paillet et al. 1985; Rider 1996).

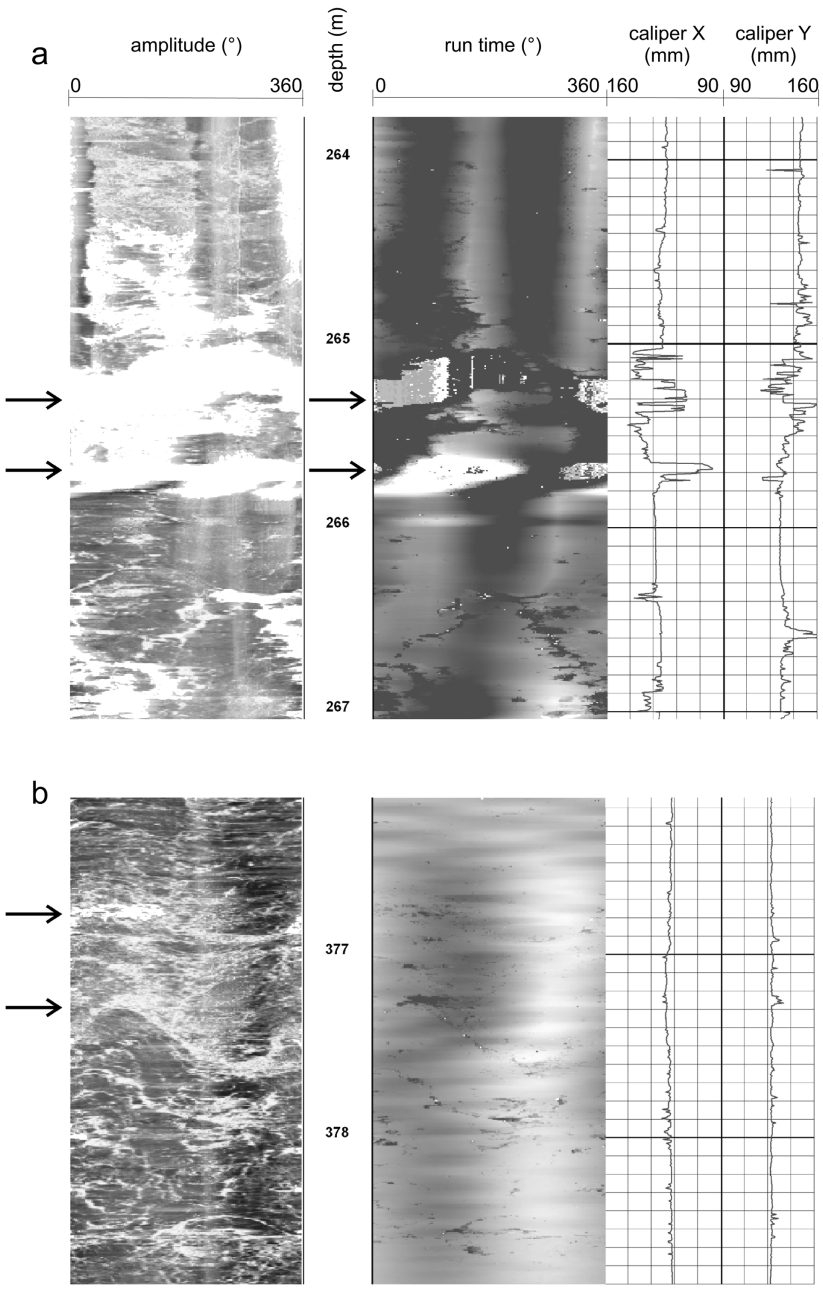

Fig. 11. Appearance of fractures (marked by horizontal arrows) in the televiewer images. a) Open fractures are characterized by a white signal both in the televiewer amplitude and run-time log. The caliper log (borehole diameter) is enhanced in this section. b) Closed fractures show a white signal in the televiewer amplitude log, but (almost) no signal in the run-time log. The caliper log is not or only slightly enhanced in this section.

Sixty-one fractures were identified with two main dip directions: southeast (~125°) and southwest (~245°) (Fig.12). The dip angle has a maximum between 50° and 70°. The vector diagram shows the variation in fracture density and orientation according to depth (Fig. 13). The fracture density increases slightly with depth and peaks between 340 and 380 m. Here, the lithology is composed of meta-graywacke with some breccia intercalations.

Main Stress Direction

An enlargement is seen on the amplitude and run-time logs as vertical stripes indicating poor reflections and long travel times or lost signals (Paillet and Kim 1987). The process of drilling a borehole concentrates stresses around the borehole wall (Zoback et al. 1985) and below the bit (Li and Schmitt 1997). Where the compressive stress concentration around the wall of the hole is larger than the rock strength, the

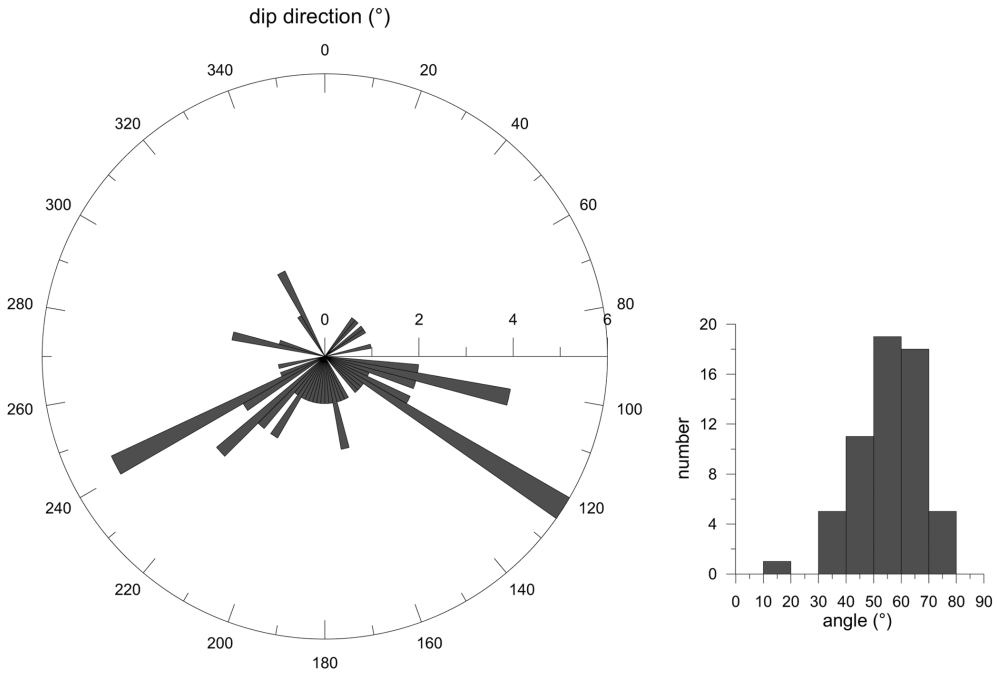

Fig. 12. An overview of all fractures observed in the televiewer images in the 238–455 m depth section. The rose diagram shows the two main strike directions. The histogram shows the distribution of the fracture dips.

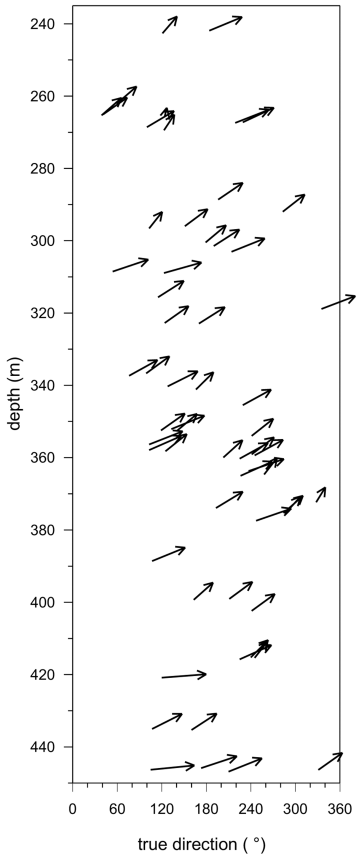

Fig. 13. Depth distributions of fracture dip direction and dip angle. The location of the arrows shows the dip direction of the fracture, the orientation of the arrow line reflects the dip angle of the fracture.

rock fails and caves into the hole, forming a borehole breakout (Gough and Bell 1981). Breakouts form on opposite sides of a hole and can be detected with 4-arm caliper logs if they are large enough, and with imaging tools such as a televiewer even when they are too small to be detected by caliper logs (Moos et al. 2000). Several vertical stripes in the televiewer logs are observed at depth intervals 256–265 m, 338–342 m, and 345–349 m (Fig. 14). Two stripes occur, one at 70°, 80°, or 90°, and another at 260° or 270°. Additionally, the two caliper logs also differ in these sections because of the borehole breakouts. By definition, the main stress direction is orthogonal to the east-west direction, and is thus oriented north-south.

CONCLUSIONS

Televiewer images were acquired in borehole LB-08A from depth 237 to 447 m, which was drilled on the outer flank of the central uplift of the Bosumtwi impact crater, Ghana. The televiewer images are a useful tool for determining structural features in their borehole orientation, differentiating in situ and drilling/logging-induced properties, and analyzing the main local stress direction. The different lithologies can be characterized by their specific physical properties based on the interpretation of wireline logs using discriminance analysis statistics. Surprisingly, those sections with a low core recovery only partly coincide with those characterized by an increased borehole diameter. One reason might be that highly fragmented and less lithified core was washed away during drilling. Another reason might be different stages of breccia alteration: fresh, unconsolidated, and altered.

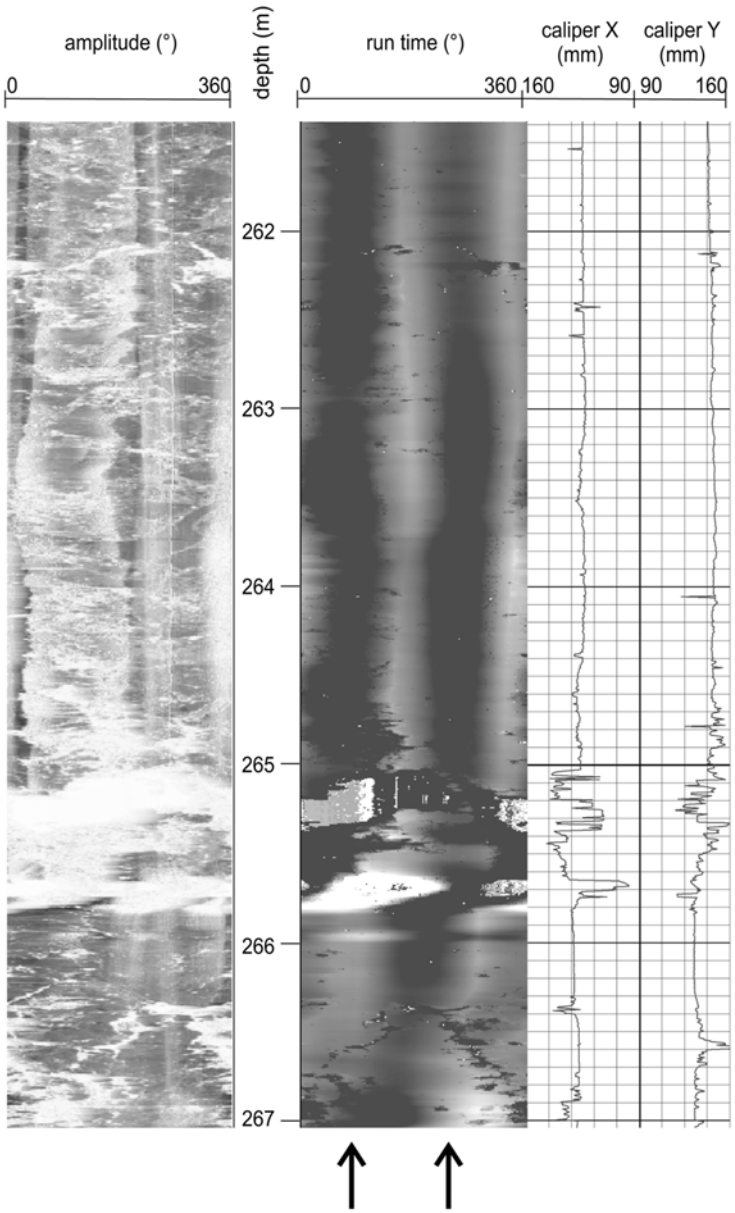

Fig. 14. Breakouts marked by vertical arrows are characterized by dark vertical stripes at about 80° and 270° in the televiewer run-time log.

Fractures are observed in the televiewer images, and we used these images to determine their characteristic structural features. The dip angle is steep (50°–70°) to southeast or southwest. Most of the fractures in the borehole are open as shown by characteristic white signals in the televiewer amplitude and run-time logs. The suggested main stress direction is north-south.

An important question regarding the Bosumtwi impact crater is whether or not effects from the impact event in the rocks are somehow reflected in the televiewer images and/or wireline logs. One method to determine this is to compare the televiewer image characteristics of a particular lithology at different borehole depths. Our investigations show no significant differences for each of the three lithologies at different depths. Characteristic features of impact rocks with increasing temperature and pressure are broken minerals, diaplectic glass, and mineral and rock melt (e.g., Deutsch and Langenhorst 1998). Other characteristic features of impact structures may be high-pressure modifications of quartz minerals (coesite and stishovite), shock metamorphism, impact breccia, and trace elements from impact bodies (e.g., platinum, iridium, and gold). Overall, it does not appear possible to use wireline logs and televiewer images in this case to differentiate the different lithologies and any influence of impact processes. The problem with interpreting the wireline logs is that they are influenced by numerous

parameters in addition to the impact event. These parameters are lithology, borehole conditions, pre-impact structures, fractures, fragmentation, and the impact event itself.

Acknowledgments–Drilling at Bosumtwi was supported by the International Continental Drilling Program (ICDP), the U.S. NSF-Earth System History Program under grant no. ATM-0402010, the Austrian FWF (project P17194-N10), the Austrian Academy of Sciences, and by the Canadian NSERC. Drilling operations were performed by DOSECC.

This research was supported by the German Research Foundation (WO672/5-1). We thank Thomas Röckel (Bayreuth) for helpful ideas regarding the interpretation of televiewer images. We would like to say thanks to Sabine Luetke and Alex Deutsch (Muenster) for discussions and explanations regarding impact crater studies. Finally, we would like to thank the two anonymous reviewers and the co-editors of this volume Christian Koeberl, Uwe Reimold, and Bernd Milkereit, who helped to improve the paper a lot.

Editorial Handling—Dr. Bernd Milkereit

REFERENCES

Backhaus K., Erikson B., Plinke W., Schuchard-Ficher C., and Weiber R. 1996. *Multivariate Analysemethoden: Eine anwendungsorientierte Einführung*, 5 Auflage. Berlin: Springer-Verlag. 591 p.

Coney L., Reimold W. U., Koeberl C., and Gibson R. L. 2006. Mineralogical and geochemical investigations of impact breccias in the ICDP borehole LB-07A, Bosumtwi impact structure, Ghana (abstract #1279). 37th Lunar and Planetary Science Conference. CD-ROM.

Deutsch A. and Langenhorst F. 1998. Mineralogy of astroblemes—Terrestrial impact craters. In *Advanced mineralogy,* vol. 3, edited by Marfunin A. S. Berlin: Springer-Verlag. pp. 76–95.

Deutsch A., Heinrich V., and Luetke S. 2006. The Lake Bosumtwi impact crater drilling project (BCDP): Lithological profile of wellhole BCDP-8A (abstract #1292). 37th Lunar and Planetary Science Conference. CD-ROM.

Deutsch A., Luetke S., and Heinrich V. 2007. The ICDP Lake Bosumtwi impact crater scientific drilling project (Ghana): Core LB-08A litho-log, related ejecta, and shock recovery experiments. *Meteoritics & Planetary Science* 42. This issue.

Gough D. I. and Bell J. S. 1981. Stress orientations from borehole wall fractures with examples from Colorado, east Texas, and northern Canada. *Canadian Journal of Earth Sciences* 19:1358–1370.

Jones W. B., Bacon M., and Hastings D. A. 1981. The Lake Bosumtwi impact crater, Ghana. *Geological Society of America Bulletin* 92:342–349.

Junner N. R. 1937. The geology of the Bosumtwi caldera and surrounding country. *Gold Coast Geological Survey Bulletin* 8: 1–38.

Koeberl C. and Reimold W. U. 2005. Bosumtwi impact crater, Ghana (West Africa): An updated and revised geological map, with explanations. *Jahrbuch der Geologischen Bundesanstalt, Wien (Yearbook of the Austrian Geological Survey)* 145:31–70 (+1 map, 1:50,000).

Koeberl C., Bottomley R., Glass B. P., and Storzer D. 1997. Geochemistry and age of Ivory Coast tektites and microtektites. *Geochimica et Cosmochimica Acta* 61:1745–1772.

Leube A., Hirdes W., Mauer R., and Kesse G. O. 1990. The early Proterozoic Birimian Supergroup of Ghana and some aspects of its associated gold mineralization. *Precambrian Research* 46: 139–165.

Li Y. and Schmitt D. R. 1997. Well-bore bottom stress concentration and induced fractures. *AAPG Bulletin* 81:1909–1925.

Moos D., Jarrard R. D., Paulsen T. S., Scholz E., and Wilson T. J. 2000. Acoustic borehole televiewer results from CRP-2/2A, Victoria Land Basin, Antarctica. *Terra Antarctica* 7:279–286.

Paillet F. L. and Kim K. 1987. Character and distribution of borehole breakouts and their relationship to in situ stresses in deep Columbia River basalts. *Journal of Geophysical Research* 92: 6223–6234.

Paillet F. L., Keys W. S., and Hess A. E. 1985. Effects of lithology on televiewer-log quality and fracture interpretation. Proceedings, 27th Annual Logging Symposium, Society of Professional Well Log Analysts. pp. 1–31.

Plado J., Pesonen L. J., Koeberl C., and Elo E. 2000. The Bosumtwi meteorite impact structure, Ghana: A magnetic model. *Meteoritics & Planetary Science* 35:723–732.

Reimold W. U., Brandt D., and Koeberl C. 1997. Geological studies at Lake Bosumtwi impact crater, Ghana (abstract). *Meteoritics & Planetary Science* 32:A107.

Reimold W. U., Brandt D., and Koeberl C. 1998. Detailed structural analysis of the rim of a large, complex impact crater: Bosumtwi crater, Ghana. *Geology* 26:543–546.

Reimold W. U., Coney L., Koeberl C., and Gibson R. L. 2006. ICDP borehole LB-07A (Bosumtwi impact structure, Ghana): An overview and first multidisciplinary results (abstract #1350). 37th Lunar and Planetary Science Conference. CD-ROM.

Rider M. 1996. *The geological interpretation of well logs*. London: Whitless Publishing. 280 p.

Scholz C. A., Karp T., Brooks K., Milkereit B., Amoako P. Y. O., and Arko J. A. 2002. Pronounced central uplift identified in the Bosumtwi impact structure, Ghana, using multichannel seismic reflection data. *Geology* 30:939–942.

Schönwiese C. D. 2000. *Praktische Statistik für Meteorologen und Geowissenschaftler*, 3 Auflage. Berlin: Borntraeger. 298 p.

Serra O. and Serra L. 2003. *Well logging and geology*. Méry Corbon: Editions Serralog. 436 p.

Taylor T. J. 1991. A method for identifying fault related fracture systems using the borehole televiewer. Proceedings, 32nd Annual Symposium, Society of Petrophysicists and Well Log Analysts (SPWLA). pp. 1–19.

Ugalde H. A. 2006. Geophysical signature of small to midsize terrestrial impact structures. Ph.D. thesis, University of Toronto, Toronto, Ontario, Canada.

Zemanek J., Glenn E. E., Norton L. J., and Caldwell R. L. 1970. Formation inspection with the borehole televiewer. *Geophysics* 35:254–269.

Zoback M. D., Moos D., Mastin L., and Anderson R. N. 1985. Wellbore breakouts and in-situ stress. *Journal of Geophysical Research* 90:5523–5530.